

Group 3 Metal Complexes of Salen-like Fluorous Dialkoxy–Diimino Ligands: Synthesis, Structure, and Application in Ring-Opening Polymerization of *rac*-Lactide and *rac*- β -Butyrolactone

Ekaterina Grunova, Evgueni Kirillov, Thierry Roisnel, and Jean-François Carpentier*

Catalysis and Organometallics, UMR 6226 Sciences Chimiques de Rennes, CNRS-University of Rennes 1, 35042 Rennes Cedex, France

Received June 30, 2008

The coordination chemistry of the dianionic fluorous dialkoxy–diimino ligand $\{\text{OC}(\text{CF}_3)_2\text{-CH}_2\text{C}(\text{Me})=\text{NCH}_2\text{CH}_2\text{N}=\text{C}(\text{Me})\text{CH}_2\text{C}(\text{CF}_3)_2\text{O}\}^{2-}$ ($\{\text{ON}^{\text{Et}}\text{NO}\}^{2-}$) onto Y(III) and La(III) centers has been studied. The diimino–diol $\{\text{ON}^{\text{Et}}\text{NO}\}_2$ reacts with 1 equiv of $\text{Y}(\text{N}(\text{SiHMe}_2)_2)_3 \cdot 2\text{THF}$ to afford $\{\text{ON}^{\text{Et}}\text{NO}\}\text{Y}(\text{N}(\text{SiHMe}_2)_2)(\text{THF})$ (**1**). Complex **1** slowly decomposes in solution, forming as yet undefined products, but could be stabilized by further reaction with 1 equiv of (*R*)-(+)-*tert*-butyl lactate, to give selectively $[\{\text{ON}^{\text{Et}}\text{NO}\}\text{Y}(\text{R}-t\text{Bu-lactate})_2]$ (**2**) in 78% yield. A single-crystal diffraction study revealed that **2** is dinuclear in the solid state, with bridging $\mu, \kappa^2\text{O}, \text{O}, \text{O}$ -lactate units and tetra-coordinated $\{\text{ON}^{\text{Et}}\text{NO}\}$ units. The same geometry is retained in THF-*d*₈ solution, as indicated by ¹H, ¹³C, and ¹⁹F NMR spectroscopy. Reaction of $\{\text{ON}^{\text{Et}}\text{NO}\}_2$ with 1 equiv of $\text{La}(\text{N}(\text{SiHMe}_2)_2)_3 \cdot 2\text{THF}$ or $\text{La}(\text{N}(\text{SiMe}_3)_2)_3$ systematically yielded $\{\text{ON}^{\text{Et}}\text{NO}\}\text{La}\{\text{ON}^{\text{Et}}\text{NOH}\}$ (**3**), which was characterized by single-crystal X-ray diffraction and NMR studies. Complex **2** is an effective initiator for the controlled-“living” ring-opening polymerization of *rac*-lactide and *rac*- β -butyrolactone, giving atactic polymers with high molecular weights (M_n up to 55 000 g mol⁻¹) that match well the calculated values and relatively narrow polydispersities ($M_w/M_n = 1.06\text{--}1.60$). The immortal ROP of *rac*-lactide appears feasible by combining complex **2** with 5 equiv of 2-propanol.

Introduction

Investigation into the use of alkoxide/aryloxide ancillaries to replace ubiquitous cyclopentadienyl-type ligands in modern coordination chemistry of early transition metals (groups 3–5) has become very popular in recent years. This is largely related to the permanent search for new-generation catalysts, in particular for the polymerization of olefins and polar monomers.¹ In principle, hard, electronegative π -donor ligands such as alkoxides are attractive because they offer strong metal–oxygen bonds that are expected to stabilize complexes of these electropositive metals.^{2,3} Also, the great variety of these ligands conveniently obtained from alcohols allows considerable variation in steric and electronic features. However, the synthetic chemistry of early-transition-metal *alkoxide*-based complexes

often proved to be quite complicated. This is largely due to the high tendency of the relatively more basic alkoxide ligands (as compared to aryloxides) to act as bridging ligands, eventually resulting in (highly) agglomerated structures.

One strategy to overcome this difficulty consists of the use of highly stable fluorous tertiary alcohol ligands. Introduction of electron-withdrawing CF₃ groups α to the alkoxide generates intra- and intermolecular repulsions, as well as a less basic alkoxide O atom, and as a result, a less distinct bridging tendency is observed.² Following this line, we have recently described some bi- and tetradentate fluorous alkoxy–*amino* ligand systems that proved to be efficient for preparing discrete complexes of oxophilic metal centers such as Y, Zr, and Al⁴ and in turn developing valuable catalytic applications.

We report herein the preparation and structural characterization of yttrium and lanthanum complexes^{5,6} supported by an

* To whom correspondence should be addressed. Fax: (+33)(0)223-236-939. E-mail: jean-francois.carpentier@univ-rennes1.fr.

(1) For reviews on post-metallocene complexes of groups 3–5 and the lanthanides related to polymerization, see: (a) Britovsek, G. J. P.; Gibson, V. C.; Wass, D. F. *Angew. Chem., Int. Ed.* **1999**, *38*, 428. (b) Edelmann, F. T.; Freckmann, D. M. M.; Schumann, H. *Chem. Rev.* **2002**, *102*, 1851. (c) Gibson, V. C.; Spitzmesser, S. K. *Chem. Rev.* **2003**, *103*, 283. (d) Gromada, J.; Morteux, A.; Carpentier, J.-F. *Coord. Chem. Rev.* **2004**, *248*, 397. (e) Corradini, P.; Guerra, G.; Cavallo, L. *Acc. Chem. Res.* **2004**, *37*, 231.

(2) (a) Bradley, D. C.; Mehrotra, R. M.; Rothwell, I. P.; Singh, A. *Alkoxo and Aryloxo Derivatives of Metals*; Academic Press: London, 2001. (b) Mehrotra, R. M.; Singh, A. *Prog. Inorg. Chem.* **1997**, *46*, 239. (c) Hubert-Pfalzgraf, L. G. *Coord. Chem. Rev.* **1998**, *178–180*, 967.

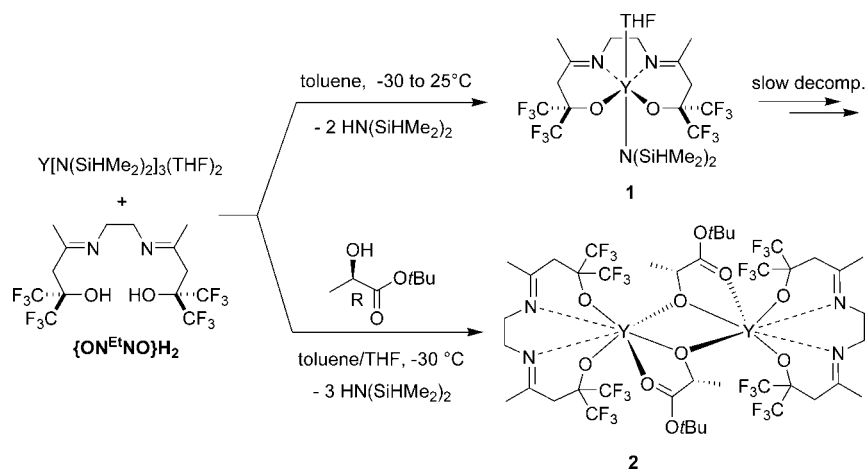
(3) For reviews on the alkoxy and aryloxo chemistry of lanthanides, see: (a) Caulton, K. G.; Hubert-Pfalzgraf, L. G. *Chem. Rev.* **1990**, *90*, 969. (b) Mehrotra, R. C.; Singh, A.; Tripathi, U. M. *Chem. Rev.* **1991**, *91*, 1287. (c) Hubert-Pfalzgraf, L. G. *New J. Chem.* **1995**, *19*, 727. (d) Anwander, R. *Top. Curr. Chem.* **1996**, *179*, 149. (e) Piers, W. E.; Emslie, D. J. H. *Coord. Chem. Rev.* **2002**, *233–234*, 131. (f) Edelmann, F. T.; Freckmann, D. M. M.; Schumann, H. *Chem. Rev.* **2002**, *102*, 1851.

(4) (a) Lavanant, L.; Chou, T.-Y.; Chi, Y.; Lehmann, C. W.; Toupet, L.; Carpentier, J.-F. *Organometallics* **2004**, *23*, 5450. (b) Amgoune, A.; Lavanant, L.; Thomas, C. M.; Chi, Y.; Welter, R.; Dagorne, S.; Carpentier, J.-F. *Organometallics* **2005**, *24*, 6279. (c) Kirillov, E.; Lavanant, L.; Thomas, C. M.; Roisnel, T.; Chi, Y.; Carpentier, J.-F. *Chem. Eur. J.* **2007**, *13*, 923.

(5) For selected examples of metal groups 3 and 4 and lanthanide complexes bearing fluorous alkoxide ligands, see: (a) Bradley, D. C.; Chudszynska, H.; Hursthouse, M. B.; Motevalli, M. *Polyhedron* **1994**, *12*, 1907. (b) Bradley, D. C.; Chudszynska, H.; Hursthouse, M. B.; Motevalli, M. *Polyhedron* **1994**, *13*, 7. (c) Samuels, J. A.; Lobkovsky, E. B.; Streib, W. E.; Foltling, K.; Huffman, J. C.; Zwanziger, J. W.; Caulton, K. G. *J. Am. Chem. Soc.* **1993**, *115*, 5093. (d) Tsukuhara, T.; Swenson, D. C.; Jordan, R. F. *Organometallics* **1997**, *16*, 3303.

(6) Fluorous alkoxy–imino ligands were first prepared in the coordination sphere of metal ions, i.e. Cu²⁺, Ni²⁺, Co²⁺, Ce³⁺, and Ce⁴⁺, by the template condensation of primary (di)amines with the fluorous β -ketol MeC(=O)CH₂C(CF₃)₂OH; see: (a) Martin, J. W. L.; Willis, C. J. *Can. J. Chem.* **1977**, *55*, 2459. (b) Konefal, E.; Loeb, S. J.; Stephan, D. W.; Willis, C. J. *Inorg. Chem.* **1984**, *23*, 538.

Scheme 1



original tetradentate ethylene-bridged fluororous dialkoxy-*diimino* ligand, $\{\text{OC}(\text{CF}_3)_2\text{CH}_2\text{C}(\text{Me})=\text{NCH}_2\text{CH}_2\text{N}=\text{C}(\text{Me})\text{CH}_2\text{C}(\text{CF}_3)_2\text{O}\}^{2-}$ ($\{\text{ON}^{\text{Et}}\text{NO}\}^{2-}$), which we recently designed.⁷ Preliminary studies on the catalytic performances of such discrete complexes in the ROP of racemic lactide and racemic β -butyrolactone are also reported.

Results and Discussion

Synthesis and Characterization of Fluorous Diolate-*Diimino* Yttrium and Lanthanum Complexes. The amine elimination reaction between $\text{Y}(\text{N}(\text{SiHMe}_2)_2)_3 \cdot 2\text{THF}$ and 1 equiv of the proligand $\{\text{ON}^{\text{Et}}\text{NO}\}\text{H}_2$ proceeds immediately at -30°C , equally in benzene or toluene, to afford the corresponding monoamido complex $\{\text{ON}^{\text{Et}}\text{NO}\}\text{Y}(\text{N}(\text{SiHMe}_2)_2)(\text{THF})$ (**1**), with concomitant release of 2 equiv of bis(dimethylsilyl)amine (Scheme 1). Compound **1** is readily soluble in the usual organic solvents (THF, benzene, and toluene) and was authenticated by multinuclear NMR (vide infra). However, complex **1** decomposes in such solutions, at ambient temperature over days, with liberation of $\text{HN}(\text{SiHMe}_2)_2$ (identified by NMR); the yttrium coproduct(s) eventually formed in this process could not be identified thus far.⁸ We also observed that prolonged exposure of solid **1** under high vacuum resulted in the loss of the coordinated THF molecule and the formation of poorly soluble, as yet undefined products. The above observations contrast markedly with the stability (under similar conditions) of the related fluororous diolate-*diamino* complex $\{\text{CH}_2\text{NMeCH}_2\text{C}(\text{CF}_3)_2\text{O}\}_2\text{Y}(\text{N}(\text{SiHMe}_2)_2)(\text{THF})$,^{4a} which was synthesized following an amine elimination protocol analogous to that used for **1**, but under harsher conditions (60°C in THF). It is not clear yet at this time whether this dramatic change in stability is related to the difference in the size of metallacycles (six- vs five-membered, respectively) and/or the replacement of imino for amino donor groups.

Due to the instability of complex **1** in solution and the resulting impossibility to get suitable crystals for X-ray diffraction analysis, **1** was characterized by multinuclear NMR spectroscopy in toluene- d_8 at room temperature, using a freshly

prepared sample. Key ^1H NMR data include one AB system for the $\text{CH}_2\text{C}=\text{N}$ moieties, another AB system for the CHHCHH bridge, and one singlet for the methyl groups. The $^{19}\text{F}\{^1\text{H}\}$ NMR spectrum of **1** displays two sharp quartets of equal intensity, indicating that the two CF_3 groups within each $\text{C}(\text{CF}_3)_2$ moiety are magnetically nonequivalent. Also, single resonances for the methyl, imino $\text{N}=\text{C}$, methylene(imino), and ethylene bridge carbon atoms, respectively, are observed in the ^{13}C NMR spectrum. These features are consistent with an overall C_2 symmetry of complex **1** in toluene solution, which contrasts with the C_1 symmetry observed for the related fluororous diolate-*diamino* complex $\{\text{CH}_2\text{NMeCH}_2\text{C}(\text{CF}_3)_2\text{O}\}_2\text{Y}(\text{N}(\text{SiHMe}_2)_2)(\text{THF})$.^{4a} We assume that, thanks to the rigidity brought by the two imino functions, the $\{\text{ON}^{\text{Et}}\text{NO}\}$ ligand likely adopts a planar coordination, in a Salen-like fashion⁹ (Scheme 1). Alternatively, the $\{\text{ON}^{\text{Et}}\text{NO}\}$ ligand could adopt a helicoidal wrapping around the metal center, with both alkoxides located at apical positions. However, 2D NMR could not unambiguously distinguish between these two possibilities.

In order to stabilize yttrium complexes of the $\{\text{ON}^{\text{Et}}\text{NO}\}$ ligand, complex **1** was generated in situ at -30°C and treated with 1 equiv of (*R*)-(+)-*tert*-butyl lactate (introduced simultaneously with the precursors of **1**) (Scheme 1). This one-pot procedure offered cleanly the corresponding lactate complex (**2**), which crystallized out of the reaction mixture at low temperature and was thus isolated in high yield (78%). **2** is a rare example of a discrete group 3 metal lactate complex, which relates to the $1,\omega$ -dithiaalkanediyl-bridged bisphenolato (OSSO)-type $[(\text{OSSO})\text{Sc}((\text{R})\text{-tert-Bu lactate})]_2$ complex recently described by Okuda¹⁰ and which is of direct relevance to active species in the ROP of lactide (vide infra).¹¹ Complex **2** is highly soluble in THF and somewhat less soluble in toluene and benzene. In contrast to the case for **1**, toluene and THF solutions of **2** are stable at room temperature, at least for weeks.

Single crystals of **2** suitable for X-ray diffraction analysis were obtained by recrystallization from a toluene/THF (6:1) solution at -15°C . Crystallographic data and structural determination details are summarized in Table 1, and important bond distances and angles are given in Table 2. Complex **2** adopts in the solid state a dimeric structure, similar to that of $[(\text{OSSO})$ -

(7) Marquet, N.; Grunova, E.; Kirillov, E.; Bouyahyi, M.; Thomas, C. M.; Carpentier, J.-F. *Tetrahedron* **2008**, *64*, 75.

(8) Release of free $\text{HN}(\text{SiHMe}_2)_2$ was observed by ^1H NMR (δ 0.14 ppm) after several hours in toluene- d_8 at room temperature and reached ca. 50% (vs $\text{Y}-\text{N}(\text{SiHMe}_2)_2$) after 3 days. Similar decomposition was observed from benzene- d_6 and THF- d_8 solutions. Due to the strict precautions employed for drying solvents, adventitious hydrolysis of $\text{Y}-\text{N}(\text{SiHMe}_2)_2$ was discarded and release of free $\text{HN}(\text{SiHMe}_2)_2$ is presumably attributed to a hydrogen abstraction from the ligand backbone.

(9) Atwood, D. A.; Harvey, M. J. *Chem. Rev.* **2001**, *101*, 37.

(10) Ma, H.; Spaniol, T. P.; Okuda, J. *Angew. Chem., Int. Ed.* **2006**, *45*, 7818.

(11) For other examples of discrete alkyl lactate metal complexes used as initiators for ROP of lactide, see: Chamberlain, B. M.; Cheng, M.; Moore, D. R.; Oviatt, T. M.; Lobkovsky, E. B.; Coates, G. W. *J. Am. Chem. Soc.* **2001**, *123*, 3229.

Table 1. Summary of Crystal and Refinement Data for Complexes 2 and 3

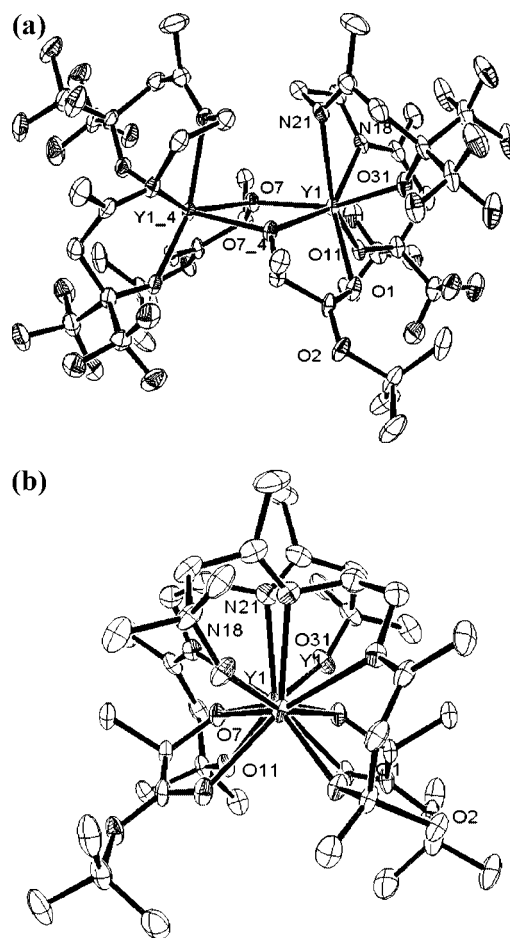
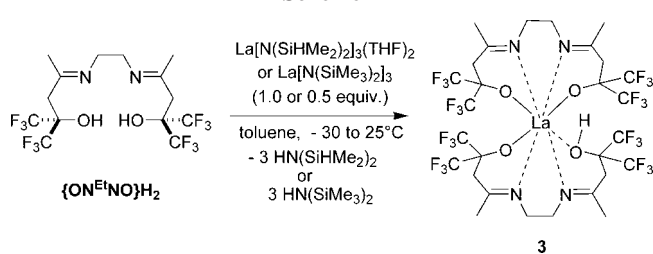
	2	3• (toluene)
empirical formula	C ₄₂ H ₅₄ F ₂₄ N ₄ O ₁₀ Y ₂	C ₃₅ H ₄₀ F ₂₄ LaN ₄ O ₄
formula wt	1408.71	1175.62
temp, K	100(2)	100(2)
wavelength, Å	0.710 73	0.710 73
cryst syst	trigonal	orthorhombic
space group	<i>P</i> 3 ₁ 2 ₁	<i>P</i> 2 ₁ 2 ₁ 2 ₁
unit cell dimens		
<i>a</i> , Å	24.6268(15)	17.5672(8)
<i>b</i> , Å	24.6268(15)	18.3588(9)
<i>c</i> , Å	11.0610(6)	27.1018(13)
<i>V</i> , Å ³	5809.5(5)	8740.7(7)
<i>Z</i>	3	8
calcd density, Mg m ⁻³	1.208	1.787
abs coeff, mm ⁻¹	1.588	1.123
cryst size, mm ³	0.6 × 0.07 × 0.03	0.5 × 0.44 × 0.41
no. of rflns collected	53 170	134 733
no. of indep rflns	8865 (<i>R</i> (int) = 0.1155)	19 939 (<i>R</i> (int) = 0.0462)
max and min transmission	0.953 and 0.386	0.631 and 0.570
no. of data/restraints/params	8865/0/370	19 939/0/1225
final <i>R</i> indices	<i>R</i> 1 = 0.0528, <i>wR</i> 2 = 0.1163	<i>R</i> 1 = 0.0292, <i>wR</i> 2 = 0.0708
<i>R</i> indices (all data)	<i>R</i> 1 = 0.0846, <i>wR</i> 2 = 0.1259	<i>R</i> 1 = 0.0321, <i>wR</i> 2 = 0.0723
goodness of fit on <i>F</i> ²	0.944	1.040
largest diff peak, e Å ⁻³	0.359 and -0.515	1.027 and -0.761

Table 2. Selected Bond Lengths (Å) and Angles (deg) for [{ON^{Et}NO}Y((*R*)-*tert*-Bu lactate)]₂ (2)

Y(1)–O(31)	2.171(3)	O(2)–C(3)	1.485(6)
Y(1)–O(11)	2.175(3)	O(7)–C(8)	1.420(5)
Y(1)–O(7)	2.309(3)	O(11)–C(12)	1.329(5)
Y(1)–O(1)	2.386(3)	C(16)–N(18)	1.272(6)
Y(1)–N(21)	2.530(4)	N(18)–C(19)	1.468(6)
Y(1)–N(18)	2.562(4)	C(20)–N(21)	1.476(6)
C(1)–O(1)	1.219(5)	N(21)–C(22)	1.275(6)
C(1)–O(2)	1.303(5)	O(31)–C(32)	1.344
O(31)–Y(1)–O(11)	104.94(11)	O(11)–Y(1)–N(21)	136.79(12)
O(31)–Y(1)–O(7)	160.41(13)	O(7)–Y(1)–N(21)	85.74(12)
O(11)–Y(1)–O(7)	90.44(11)	O(7)#1–Y(1)–N(21)	90.78(12)
O(31)–Y(1)–O(7)#1	106.40(11)	O(1)–Y(1)–N(21)	140.37(12)
O(11)–Y(1)–O(7)#1	128.49(11)	O(31)–Y(1)–N(18)	84.94(13)
O(7)–Y(1)–O(7)#1	71.46(10)	O(11)–Y(1)–N(18)	74.14(12)
O(31)–Y(1)–O(1)	80.17(13)	O(7)–Y(1)–N(18)	87.78(10)
O(11)–Y(1)–O(1)	79.09(11)	O(7)#1–Y(1)–N(18)	147.86(12)
O(7)–Y(1)–O(1)	115.24(11)	O(1)–Y(1)–N(18)	144.72(12)
O(7)#1–Y(1)–O(1)	67.42(10)	N(21)–Y(1)–N(18)	62.72(13)
O(31)–Y(1)–N(21)	74.76(13)	N(18)–Y(1)–Y(1)#1	117.02(9)

Sc((*R*)-*tert*-Bu lactate)]₂,¹⁰ with lactate units bridging the two {ON^{Et}NO}Y fragments via the O(alkoxide) atoms (Figure 1). In addition to the $\mu, \kappa^2 O, O, O$ -lactate units, the yttrium atoms bear each a κ^4 -chelated {ON^{Et}NO} ligand and, thus, are seven-coordinated. The distance of 3.740(2) Å between the yttrium atoms in the dimer is beyond significant interactions. The two Y atoms and the two bridging O atoms are almost coplanar (Y atoms lie 0.094 Å below and O atoms lie 0.094 Å above the Y–O–O–Y mean plane). The two lactate moieties point in the same direction above this plane, while both {ON^{Et}NO} chelate rings point essentially in the opposite direction, generating an exact (crystallographic) *C*₂-symmetric environment (Figure 1b).

The Y–O bond lengths involving the alkoxide atoms in the bridge (Y(1)–O(7) = 2.309(3) Å) are expectedly shorter than the Y–O bond lengths involving the carbonyl oxygens of the lactate moieties (Y(1)–O(1) = 2.386(3) Å). Those distances are longer than the corresponding ones observed in [(OSSO)-Sc((*R*)-*tert*-Bu lactate)]₂ (Y–O(alkoxide) = 2.098(4) and 2.129(4) Å; Y–O(ester) = 2.254(4) Å),¹⁰ which essentially reflects the

**Figure 1.** (a) ORTEP view of [{ON^{Et}NO}Y((*R*)-*tert*-Bu lactate)]₂ (2) with ellipsoids given at the 30% probability level (H atoms are omitted for clarity). (b) Alternative view of [{ON^{Et}NO}Y((*R*)-*tert*-Bu lactate)]₂ (2) along the Y–Y axis, showing the *C*₂ symmetry (ellipsoids are at the 30% probability level; F and H atoms are omitted for clarity).**Scheme 2**

difference in ionic radius between Y and Sc centers.¹² The Y–O and Y–N bond distances associated with the {ON^{Et}NO} fragments are each slightly different (Y(1)–O(31,11) = 2.171(3) and 2.175(3) Å; Y(1)–N(18,21) = 2.530(4) and 2.562(4) Å) and compare well with the corresponding distances observed in the diolate–*diamino* complex {CH₂NMeCH₂C(CF₃)₂-O}₂Y(N(SiHMe₂)₂)(THF) (Y–O = 2.149(2) and 2.162(2) Å; Y–N = 2.501(2) and 2.704(2) Å).^{4a}

The NMR data of 2 are consistent with the dimeric structure observed in the solid state retained in THF-*d*₈ solution. The ¹H and ¹³C NMR data (see the Experimental Section and the

(12) Effective ionic radii for six-coordinate metal centers are as follows: Sc³⁺, 0.745 Å; Y³⁺, 0.90 Å; La³⁺, 1.032 Å. See: Shannon, R. D. *Acta Crystallogr., Sect. A* **1976**, A32, 751.

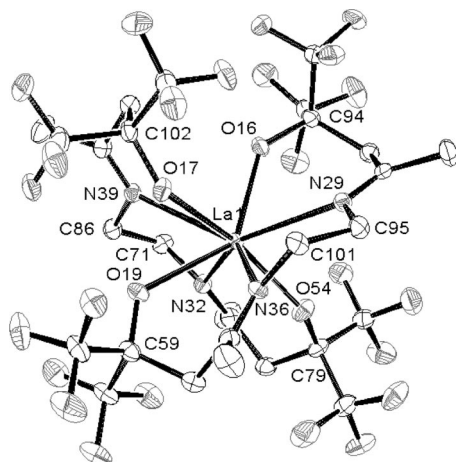


Figure 2. ORTEP view of $\{\text{ON}^{\text{Et}}\text{NO}\}\text{La}\{\text{ON}^{\text{Et}}\text{NOH}\}$ (**3**) with ellipsoids at the 50% probability level (H atoms are omitted for clarity; only molecule 1 is displayed).

Supporting Information) indicate the equivalence of both lactate units, with a global C_2 symmetry around the metal centers, as observed in $[(\text{OSSO})\text{Sc}(\text{R-tert-Bu lactate})_2]_2$.¹⁰ On the other hand, the asymmetric center in the lactate units make the chelated $\{\text{ON}^{\text{Et}}\text{NO}\}$ units dissymmetric. Thus, the $^{19}\text{F}\{^1\text{H}\}$ NMR spectrum of **2** displays four sharp quartets of equal intensity, showing that the two CF_3 groups within each $\text{C}(\text{CF}_3)_2$ moiety are nonequivalent (see the Supporting Information).

Attempts to generate the monoamido lanthanum complexes “ $\{\text{ON}^{\text{Et}}\text{NO}\}\text{La}(\text{N}(\text{SiHMe}_2)_2)(\text{THF})$ ” and “ $\{\text{ON}^{\text{Et}}\text{NO}\}\text{La}(\text{N}(\text{SiMe}_3)_2)(\text{THF})$ ” from $\{\text{ON}^{\text{Et}}\text{NO}\}_2$ and 1 equiv of the corresponding precursors $\text{La}(\text{N}(\text{SiHMe}_2)_2)_3 \cdot 2\text{THF}$ or $\text{La}(\text{N}(\text{SiMe}_3)_2)_3$, under various conditions, were unsuccessful. Also, a lactate complex could not be isolated following the procedure used above for yttrium complex **2**. Instead, in all cases, the “bis-ligand” complex $\{\text{ON}^{\text{Et}}\text{NO}\}\text{La}\{\text{ON}^{\text{Et}}\text{NOH}\}$ (**3**) formed, with concomitant release of 3 equiv of free amine (Scheme 2). It is likely that the larger ionic radius of La^{12} accounts for the apparent instability of relatively low-coordinate species, thus resulting in the observed formation of the bis-ligand complex. As expected, we observed that **3** also readily forms in high yield from the reaction of $\text{La}(\text{N}(\text{SiHMe}_2)_2)_3 \cdot 2\text{THF}$ (or $\text{La}(\text{N}(\text{SiMe}_3)_2)_3$) and 2 equiv of $\{\text{ON}^{\text{Et}}\text{NO}\}_2$. Complex **3** is poorly soluble in toluene, in which it is stable at room temperature for long time periods, allowing us to obtain single crystals suitable for X-ray diffraction.

Crystallographic data and structural determination details for **3** are summarized in Table 1. The unit cell of **3** contains two independent molecules, but their structural features (bond distances and angles) are essentially the same, so that only one of these is shown in Figure 2. Selected bond distances and angles are given in Table 3. In the solid state, the La atom in **3** is eight-coordinated by two κ^4 -chelated $\{\text{ON}^{\text{Et}}\text{NO}\}$ ligand units. The four La–N bonds are in the narrow range of 2.706(2)–2.747(2) Å (2.687(2)–2.721(2) Å, in the second molecule), reflecting their close similarity. On the other hand, three out of the four La–O bond lengths in **3** are in the range 2.269(2)–2.552(2) Å (O(16), O(19), O(54)), whereas the fourth one is somewhat longer (2.686(2) Å; O(17)) (2.305(2)–2.514(2) vs 2.729(2) Å, respectively, in the second molecule).¹³ Noteworthy, these large La–O bond distances are also associated with acute La–O–C angles: $\text{C}(102)\text{--O}(17)\text{--La}(1) = 128.97(19)^\circ$ vs $\text{C}(94)\text{--O}(16)\text{--La}(1) = 136.8(2)^\circ$, $\text{C}(59)\text{--O}(19)\text{--La}(1) = 129.4(2)^\circ$, $\text{C}(79)\text{--O}(54)\text{--La}(1) = 148.3(2)^\circ$ ($\text{C}(69)\text{--O}(24)\text{--La}(2)$

Table 3. Selected Bond lengths (Å) and Angles (deg) for the Two Independent Molecules of $\{\text{ON}^{\text{Et}}\text{NO}\}\text{La}\{\text{ON}^{\text{Et}}\text{NOH}\}$ (**3**)

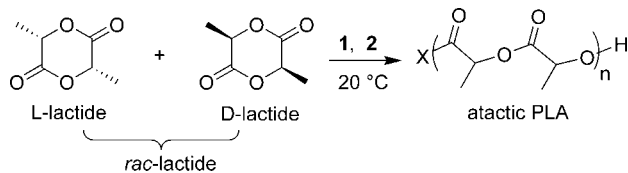
molecule 1		molecule 2	
La(1)–O(54)	2.269(2)	La(2)–O(12)	2.275(2)
La(1)–O(16)	2.305(2)	La(2)–O(10)	2.305(2)
La(1)–O(19)	2.552(2)	La(2)–O(4)	2.514(2)
La(1)–O(17)	2.686(2)	La(2)–O(24)	2.729(2)
La(1)–N(36)	2.706(2)	La(2)–N(60)	2.687(2)
La(1)–N(29)	2.711(3)	La(2)–N(72)	2.712(2)
La(1)–N(32)	2.735(3)	La(2)–N(73)	2.716(2)
La(1)–N(39)	2.747(2)	La(2)–N(80)	2.721(2)
O(16)–C(94)	1.365(4)	O(4)–C(64)	1.355(4)
O(19)–C(59)	1.371(4)	O(12)–C(70)	1.375(4)
O(17)–C(102)	1.404(4)	O(10)–C(63)	1.361(4)
O(54)–C(79)	1.345(4)	O(24)–C(69)	1.406(4)
O(54)–La(1)–O(16)	111.10(8)	O(12)–La(2)–O(10)	121.26(9)
O(54)–La(1)–O(19)	111.97(8)	O(12)–La(2)–O(4)	100.84(8)
O(16)–La(1)–O(19)	135.31(8)	O(10)–La(2)–O(4)	136.11(7)
O(54)–La(1)–O(17)	151.46(8)	O(12)–La(2)–N(60)	82.40(8)
O(16)–La(1)–O(17)	89.90(8)	O(10)–La(2)–N(60)	124.97(8)
O(19)–La(1)–O(17)	55.38(7)	O(4)–La(2)–N(60)	68.62(7)
O(54)–La(1)–N(36)	85.80(8)	O(12)–La(2)–N(72)	130.52(8)
O(16)–La(1)–N(36)	126.14(8)	O(10)–La(2)–N(72)	76.13(8)
O(19)–La(1)–N(36)	68.62(7)	O(4)–La(2)–N(72)	66.62(7)
O(17)–La(1)–N(36)	65.92(7)	N(60)–La(2)–N(72)	128.11(8)
O(54)–La(1)–N(29)	77.81(8)	O(12)–La(2)–N(73)	84.19(8)
O(16)–La(1)–N(29)	70.25(8)	O(10)–La(2)–N(73)	69.93(7)
O(19)–La(1)–N(29)	130.68(7)	O(4)–La(2)–N(73)	131.01(7)
O(17)–La(1)–N(29)	92.31(7)	N(60)–La(2)–N(73)	63.80(8)
N(36)–La(1)–N(29)	63.98(8)	N(72)–La(2)–N(73)	141.29(8)
O(54)–La(1)–N(32)	70.29(8)	O(12)–La(2)–N(80)	70.20(8)
O(16)–La(1)–N(32)	96.30(8)	O(10)–La(2)–N(80)	87.18(8)
O(19)–La(1)–N(32)	87.31(8)	O(4)–La(2)–N(80)	96.69(8)
O(17)–La(1)–N(32)	128.24(7)	N(60)–La(2)–N(80)	146.09(8)
N(36)–La(1)–N(32)	136.89(8)	N(72)–La(2)–N(80)	64.61(8)
N(29)–La(1)–N(32)	138.00(8)	N(73)–La(2)–N(80)	129.74(9)
O(54)–La(1)–N(39)	135.66(8)	O(12)–La(2)–O(24)	145.91(7)
O(16)–La(1)–N(39)	73.73(8)	O(10)–La(2)–O(24)	89.44(7)
O(19)–La(1)–N(39)	67.51(7)	O(4)–La(2)–O(24)	55.50(7)
O(17)–La(1)–N(39)	67.43(7)	N(60)–La(2)–O(24)	66.70(7)
N(36)–La(1)–N(39)	128.41(7)	N(72)–La(2)–O(24)	66.98(7)
N(29)–La(1)–N(39)	138.47(8)	N(73)–La(2)–O(24)	94.21(7)
N(32)–La(1)–N(39)	65.38(8)	N(80)–La(2)–O(24)	130.83(7)

$= 128.26(18)^\circ$ vs $\text{C}(64)\text{--O}(4)\text{--La}(2) = 129.88(19)^\circ$, $\text{C}(63)\text{--O}(10)\text{--La}(2) = 137.29(19)^\circ$, $\text{C}(70)\text{--O}(12)\text{--La}(2) = 143.0(2)^\circ$ in the second molecule).¹³ Overall, these data are consistent with the presence of one hydroxyl group, though the corresponding hydrogen atom could not be precisely located in the crystal structure, likely due to its partial delocalization.

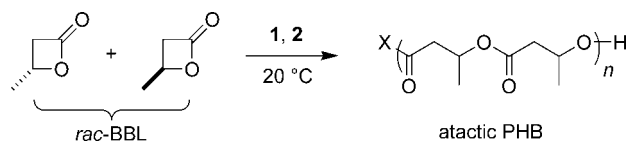
The ^1H NMR spectrum of **3** in toluene- d_8 at room temperature shows the presence of one hydroxyl proton deshielded at δ 12.46 ppm. In addition, a single series of resonances for magnetically equivalent $\{\text{ON}^{\text{Et}}\text{NO}\}$ ligands is observed. In particular, the hydrogens of the ethylene bridge of both ligand units in **3**, as well as the methylene hydrogens of the four $\text{CH}_2\text{C}=\text{N}$ fragments, appear each as one singlet at δ 3.07 and 2.61 ppm, respectively. These features are confirmed in the ^{13}C and ^{19}F NMR spectra, the latter spectrum containing only one sharp signal, indicating that all eight CF_3 groups in the complex are equivalent. These observations suggest a very rapid (on the

(13) Typical La–O bond distances and La–O–C bond angles for σ -coordinated terminal alkoxides in La complexes are as follows. Hexakis(μ_2 -2-propoxo)hexakis(2-propoxy) bis(2-propanol)dialuminumdilanthanum(III): La–O(iPr), 2.185 Å; La–O–C, 122.20°. Typical La–O(H) bond distances and La–O(H)–C bond angles for a σ -coordinated terminal alcohol in La complexes are as follows. Hexakis(μ_2 -2-propoxo)hexakis(2-propoxy)bis(2-propanol)dialuminumdilanthanum(III): La–O(H), 2.647 Å; La–O–C, 174.66°. See: Manning, T. D.; Loo, Y. F.; Jones, A. C.; Aspinall, H. C.; Chalker, P. R.; Bickley, J. F.; Smith, L. M.; Critchlow, G. W. *J. Mater. Chem.* **2005**, *15*, 3384.

Scheme 3



Scheme 4



NMR time scale) delocalization of the proton among the four oxygen atoms of the two ligand units at room temperature.

Ring-Opening Polymerization of *rac*-Lactide and *rac*- β -Butyrolactone. Discrete group 3 metal complexes are well-established catalysts–initiators for the ring-opening polymerization (ROP) of lactones and related monomers,^{14,15} such as lactide (LA) and β -butyrolactone (BBL).¹⁶ Performances, namely activity, productivity, degree of control/livingness, and stereoselectivity in the case of chiral monomers, depend crucially on ancillary ligands that define the sterics and electronics around the active metal center. We were therefore interested in evaluating the performances of the new fluororous diolate–diimino complexes prepared, considering that (i) yttrium complexes **1** and **2** possess a potentially active nucleophilic group (i.e., amido and lactate, respectively) and (ii) lactate complex **2** is assumed to be an early intermediate in the ROP of lactide or, more exactly, to mimic the active species with a growing PLA chain in such a process.¹⁰

Complexes **1** and **2** were thus assessed in the ROP of *rac*-lactide (Scheme 3) and *rac*- β -butyrolactone (Scheme 4). Representative results are summarized in Table 4. Polymerizations with complex **1** were conducted by adding a THF solution of the monomer to a freshly prepared solution of **1**, generated in situ in toluene from the precursors (vide supra).

(14) (a) Dechy-Cabaret, O.; Martin-Vaca, B.; Bourissou, D. *Chem. Rev.* **2004**, *104*, 6147. (b) O'Keefe, B. J.; Hillmyer, M. A.; Tolman, W. B. *Dalton Trans.* **2001**, 2215.

(15) (a) Aubrecht, K. B.; Chang, K.; Hillmyer, M. A.; Tolman, W. B. *J. Polym. Sci. A: Polym. Chem.* **2001**, *39*, 284. (b) Giesbrecht, G. R.; Whitener, G. D.; Arnold, J. *Dalton Trans.* **2001**, 923. (c) Oviitt, T. M.; Coates, G. W. *J. Am. Chem. Soc.* **2002**, *124*, 1316. (d) Satoh, Y.; Ikitake, N.; Nakayama, Y.; Okuno, S.; Yasuda, H. *J. Organomet. Chem.* **2003**, *667*, 42. (e) Cai, C.-X.; Amgoune, A.; Lehmann, C. W.; Carpentier, J.-F. *Chem. Commun.* **2004**, 330. (f) Zhang, L.; Shen, Z.; Yu, C.; Fan, L. *J. Macromol. Sci.* **2004**, *A41*, 927. (g) Ma, H.; Okuda, J. *Macromolecules* **2005**, *38*, 2665. (h) Bonnet, F.; Cowley, A. R.; Mountford, P. *Inorg. Chem.* **2005**, *44*, 9046. (i) Amgoune, A.; Thomas, C. M.; Roisnel, T.; Carpentier, J.-F. *Chem. Eur. J.* **2006**, *12*, 169. (j) Westmoreland, I.; Arnold, J. *Dalton Trans.* **2006**, 4155. (k) Liu, X.; Shang, X.; Tang, T.; Hu, N.; Pei, F.; Cui, D.; Chen, X.; Jing, X. *Organometallics* **2007**, *26*, 2747. (l) Binda, P. I.; Delbridge, E. E. *Dalton Trans.* **2007**, 4685. (m) Wang, J.; Cai, T.; Yao, Y.; Shen, Q. *Dalton Trans.* **2007**, 5275. (n) Wang, S.; Wang, S.; Zhou, S.; Yang, G.; Luo, W.; Hu, N.; Zhou, Z.; Song, H.-B. *J. Organomet. Chem.* **2007**, *692*, 2099. (o) Zhou, S.; Wang, S.; Sheng, E.; Zhang, L.; Yu, Z.; Xi, X.; Chen, G.; Luo, W.; Li, Y. *Eur. J. Inorg. Chem.* **2007**, 1519. (p) Zhou, H.; Guo, H.; Yao, Y.; Zhou, L.; Sun, H.; Sheng, H.; Zhang, Y.; Shen, Q. *Inorg. Chem.* **2007**, *46*, 958. (q) Gamer, M. T.; Roesky, P. W.; Pallard, I.; Le Hellaye, M.; Guillaume, S. M. *Organometallics* **2007**, *26*, 651. (r) Delbridge, E. E.; Dugah, D. T.; Nelson, C. R.; Skelton, B. W.; White, A. H. *Dalton Trans.* **2007**, 143. (s) Skvortsov, G. G.; Yakovenko, M. V.; Castro, P. M.; Fukin, G. K.; Cherkasov, A. V.; Carpentier, J.-F.; Trifonov, A. A. *Eur. J. Inorg. Chem.* **2007**, 3260. (t) Amgoune, A.; Thomas, C. M.; Carpentier, J.-F. *Pure Appl. Chem.* **2008**, *79*, 2013.

(16) (a) Amgoune, A.; Thomas, C. M.; Ilinca, S.; Roisnel, T.; Carpentier, J.-F. *Angew. Chem., Int. Ed.* **2006**, *45*, 2782. (b) Ajellal, N.; Lyubov, D. M.; Sinenkov, M. A.; Fukin, G. K.; Cherkasov, A. V.; Thomas, C. M.; Carpentier, J.-F.; Trifonov, A. A. *Chem. Eur. J.* **2008**, *14*, 5440.

Both complexes **1** and **2** are active in the ROP of *rac*-LA at ambient temperature. However, **2** proved to be significantly more active than **1** (compare entries 1 and 2 vs entries 3–17). We assume that this difference in apparent catalytic activity reflects more the higher nucleophilicity of the lactate group as initiating group (as compared to amido),^{15g,i,16} rather than the aforementioned instability of **1**, since decomposition of the latter complex is significant only after several hours.⁸ Lactate complex **2** was therefore selected for more in-depth investigations.¹¹ With this initiator system, complete conversion of 250 and 500 equiv of *rac*-LA is achieved within ca. 50 and 100 min, respectively (entries 3–17). The reaction kinetics, under these conditions, feature a pseudo-first-order dependence in lactide concentration (Figure 3).

The PLAs produced by **1** and **2** show an atactic microstructure, as revealed from the homodecoupled ¹H NMR spectra of the methine region.¹⁷ However, the polymerizations of *rac*-lactide promoted by **2** appear to be well-controlled. The linear dependence of number-average molecular weight values determined by GPC ($M_n(\text{exptl})$) on the monomer conversion for different monomer loadings is illustrated in Figure 4. Also, the experimental M_n values are in quite good agreement with the calculated values ($M_n(\text{calcd})$) up to 60 000 g/mol, assuming growth of one polymer chain per Y–lactate moiety (Table 4). Moreover, the molecular weight distributions are relatively narrow ($M_w/M_n < 1.12–1.28$ for a lactide conversion <90% at [*rac*-LA]/[Y] = 250). These results are consistent with a “controlled-living” polymerization model. The somewhat larger polydispersities observed when the polymerization reaches completion (lactide conversion >90%), with concomitant decrease of the molecular weights (compare entries 8–10), as well as for larger monomer loadings ($M_w/M_n = 1.06–1.59$ for a lactide conversion <90% at [*rac*-LA]/[Y] = 500), suggest that transesterification reactions take place.¹⁸ This hypothesis was confirmed by a MALDI-TOF-MS analysis of the produced PLAs, which indeed feature a 72 Da repeat unit.

When *rac*-LA was polymerized with **2** in the presence of 2-propanol ([*i*PrOH]/[Y] = 5, [*rac*-LA]/[Y] = 500; Table 4, entries 18 and 19), the number-average molecular weights of the resulting PLAs decreased significantly. A simple calculation from the experimental M_n values indicate that, under such conditions, extra polymer chains are created to the same extent as equivalents of 2-propanol introduced; i.e., an immortal polymerization takes place thanks to extra alcohol molecules that act as transfer agents.^{15g,18a,19} Analysis by ¹H NMR spectroscopy of the low-molecular-weight PLAs obtained under such conditions showed clearly the existence of HOCH(CH₃)CO– and isopropoxy end groups,²⁰ thus supporting the transfer process.

We also have found that, in contrast to amido complex **1**, which is inactive, lactate complex **2** is an active catalyst/initiator for the ROP of racemic β -butyrolactone (*rac*-BBL) at 20 °C (Table 4, entries 20–25). As previously observed in this type of polymerization with a rare earth catalyst system, the activity strongly depends on the solvent nature:¹⁶ the polymerization

(17) Thakur, K. A. M.; Kaen, R. T.; Hall, E. S. *Anal. Chem.* **1997**, *69*, 4303.

(18) (a) Martin, E.; Dubois, P.; Jerome, R. *Macromolecules* **2000**, *33*, 1530. (b) Stevels, W. M.; Ankone, M. J. K.; Dijkstra, P. J.; Feijen, J. *Macromolecules* **1996**, *29*, 8296. (c) Stevels, W. M.; Ankone, M. J. K.; Dijkstra, P. J.; Feijen, J. *Macromolecules* **1996**, *29*, 6132.

(19) Amgoune, A.; Thomas, C. M.; Carpentier, J.-F. *Macromol. Rapid Commun.* **2007**, *28*, 693.

(20) Save, M.; Schappacher, M.; Soum, A. *Macromol. Chem. Phys.* **2002**, *203*, 889.

Table 4. ROP of *rac*-Lactide and *rac*- β -Butyrolactone Initiated by Complexes **1** and **2**^a

entry	compd	monomer (M)	[M]/[Y]	time (min)	solvent	conversion (mol %)	$M_n(\text{calcd})^b$ (kDa)	$M_n(\text{exptl})^c$ (kDa)	M_w/M_n^c
1	1	<i>rac</i> -LA	100	60	tol/THF	90	13.0	10.2	1.33
2 ^d	1	<i>rac</i> -LA	100	120	tol/THF	100	14.4	12.3	1.48
3	2	<i>rac</i> -LA	250	3	THF	35	12.6	13.9	1.12
4	2	<i>rac</i> -LA	250	7	THF	55	19.8	17.1	1.14
5	2	<i>rac</i> -LA	250	10	THF	68	24.5	25.6	1.18
6	2	<i>rac</i> -LA	250	16	THF	85	30.6	33.4	1.25
7	2	<i>rac</i> -LA	250	24	THF	92	33.2	35.6	1.28
8	2	<i>rac</i> -LA	250	32	THF	95	34.2	37.0	1.29
9	2	<i>rac</i> -LA	250	42	THF	96	34.6	36.4	1.38
10	2	<i>rac</i> -LA	250	52	THF	97	35.0	35.0	1.42
11	2	<i>rac</i> -LA	500	3	THF	13	9.4	7.1	1.06
12	2	<i>rac</i> -LA	500	7	THF	23	16.6	13.0	1.11
13	2	<i>rac</i> -LA	500	10	THF	31	22.3	19.3	1.12
14	2	<i>rac</i> -LA	500	16	THF	52	37.5	28.7	1.26
15	2	<i>rac</i> -LA	500	35	THF	75	53.3	35.1	1.43
16	2	<i>rac</i> -LA	500	80	THF	90	60.5	43.5	1.59
17	2	<i>rac</i> -LA	500	100	THF	95	62.7	54.7	1.64
18 ^e	2	<i>rac</i> -LA	500	30	THF	66	9.5	7.8	1.21
19 ^e	2	<i>rac</i> -LA	500	60	THF	87	12.5	11.3	1.55
20	1	<i>rac</i> -BBL	100	120	toluene	0	—	—	—
21	1	<i>rac</i> -BBL	100	4300	toluene	10	0.9	nd	nd
22	2	<i>rac</i> -BBL	50	90	THF	85	3.7	nd	nd
23 ^d	2	<i>rac</i> -BBL	50	900	THF	100	4.3	2.6	1.22
24 ^d	2	<i>rac</i> -BBL	250	1000	THF	100	21.5	19.3	1.37
25	2	<i>rac</i> -BBL	250	1000	toluene	33	8.3	6.2	1.28

^a All reactions were carried out at 20 °C with $[\textit{rac}\text{-LA}]_0 = 1.0$ mol/L or $[\textit{rac}\text{-BBL}]_0 = 2.5\text{--}3.0$ mol/L. ^b Calculated M_n values considering one polymer chain per Y center. ^c Experimental M_n and M_w/M_n values determined by GPC in THF vs PS standards, corrected with 0.59 and 0.68 Mark–Houwink factors for PLAs and PHBs, respectively. ^d The reaction time was not optimized. ^e The polymerization was carried out in the presence of 5 equiv of *i*PrOH vs Y.

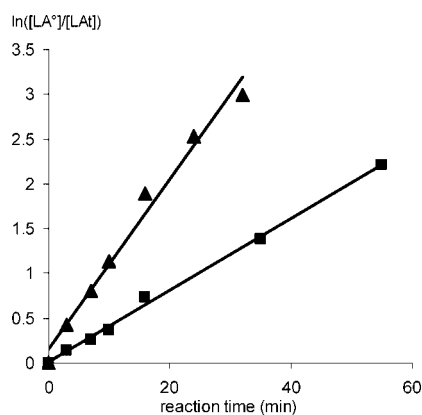


Figure 3. Pseudo-first-order kinetics of the ROP of *rac*-lactide promoted by **2** (Table 4, entries 3–17): (■) $[\text{LA}]/[\text{Y}] = 250$; (▲) $[\text{LA}]/[\text{Y}] = 500$. Pseudo-first-order rate constants are 0.11 and 0.03 mol L⁻¹ min⁻¹, respectively.

of 50 equiv of *rac*-BBL in THF reached 85% conversion in 90 min (TOF = 28 h⁻¹), while at $[\textit{rac}\text{-BBL}]/[\text{Y}] = 250$ in toluene, the conversion reached only 33% in 16 h (TOF = 5 h⁻¹). ¹³C NMR analysis of the polymers obtained showed carbonyl signals of equal intensity for racemic and meso diads, indicating the formation of atactic PHB.^{16a,21} On the other hand, the PHBs produced with **2** have relatively narrow molecular weight distribution ($M_w/M_n = 1.22\text{--}1.37$) and the experimental (corrected) number-average molecular weights are in close agreement with the calculated values. The data evidence again a significant degree of control over the polymerization.

Overall, the performance of **2** in terms of control over the molecular weights of the polymers and molecular weight distributions compare well those of related alkoxide yttrium(III) complexes supported by bis(phenolate)-type ligands having

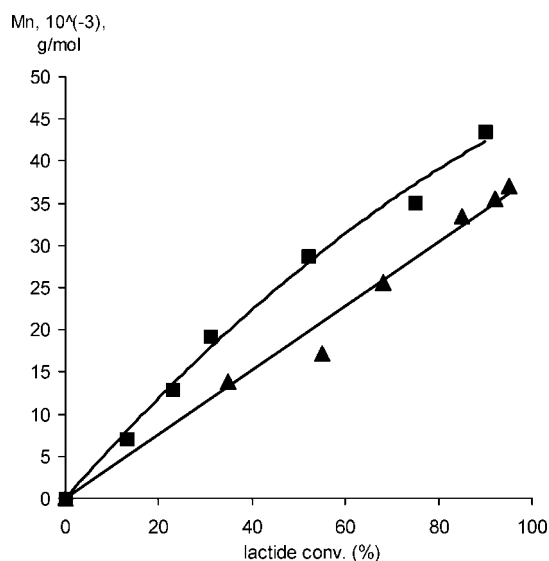


Figure 4. Dependence of the number-average molecular weights on monomer conversions in the ROP of *rac*-lactide promoted by complex **2** (Table 4, entries 3–17): (▲) $[\text{LA}]/[\text{Y}] = 250$; (■) $[\text{LA}]/[\text{Y}] = 500$.

additional donor atoms (N, O, S), such as those reported by Okuda^{10,15g} and our group.^{15e,i,t,16a} The catalytic activity of **2**, although quite significant since ROP of both *rac*-lactide and *rac*-BBL proceeds at room temperature, appears however to be somewhat lower than with these bis(phenolate)–yttrium alkoxide complexes. This might reflect the lower nucleophilicity of the lactate unit, possibly as an indirect influence of the strong electron withdrawal of the fluorine dialkoxide–diimino ligand. The most remarkable difference remains the degree of stereocontrol achieved in the ROP of racemic cyclic esters: complex **2** offers only atactic PLAs and PHBs, while yttrium alkoxide complex supported amino–alkoxy–bis(phenolate) ligands lead to highly heterotactic PLAs^{15e,i,t} and highly syndiotactic

(21) Kemnitzer, J. E.; McCarthy, S. P.; Gross, R. A. *Macromolecules* **1993**, *26*, 1221, and references cited therein.

PHBs.^{15t,16a} These observations further confirm the crucial role of ancillary ligands in chain-end stereocontrolled ROP processes.

Conclusions

The preparation of discrete group 3 metal complexes based on the salen-like tetradentate fluororous dialkoxy–diimino ligand $\{\text{ON}^{\text{Et}}\text{NO}\}^{2-}$ has been achieved using straightforward procedures. A rare yttrium complex that contains lactate moieties has been isolated and characterized in the solid state and in solution. This complex mimics the early intermediate and active species with a growing polymer chain in lactide ring-opening polymerization. In fact, this complex has been shown to be an active catalyst/initiator for the controlled ROP of both lactide and β -butyrolactone. This process is also operative in the presence of excess 2-propanol to achieve chain transfer and so-called immortal ROP of lactide.

The many possibilities to tune such fluorinated alkoxide–imino ligands⁷ open avenues for designing and preparing new series of group 3 metal complexes. Results of ongoing studies on the coordination chemistry of these original ligands with oxophilic metal centers and the application of these discrete complexes in catalysis will be reported in due course.

Experimental Section

General Procedures. All manipulations were performed under argon using standard high-vacuum Schlenk techniques or in a glovebox (<1 ppm O₂, 5 ppm of H₂O). Toluene and THF were freshly distilled under argon from sodium/benzophenone ketyl and were condensed under vacuum prior to use. Deuterated solvents (>99.5% D, Eurisotop) were freshly distilled from K_(met) under argon and degassed prior to use. 1,1,1-Trifluoro-4-[(2-[[4,4,4-trifluoro-3-hydroxy-1-methyl-3-(trifluoromethyl)butylidene]amino]ethyl)imino]-2-(trifluoromethyl)pentan-2-ol ($\{\text{ON}^{\text{Et}}\text{NO}\}_2$),⁷ Y(N(SiHMe₂)₂)₃·2THF,²² La(N(SiMe₃)₂)₃,²² and La(N(SiHMe₂)₂)₃·2THF²² were synthesized according to the reported procedures. (*R*)-(+)-*tert*-Butyl lactate (>99% GLC) was purchased from Fluka and used as received. *rac*-Lactide (Aldrich) was recrystallized from dry methanol and toluene and sublimed under vacuum at 50 °C. *rac*- β -Butyrolactone (Aldrich) was freshly distilled from CaH₂ under argon and degassed thoroughly by freeze–thaw–vacuum cycles.

NMR spectra were recorded on Bruker Avance DPX-200, AM-300, and AM-500 spectrometers in Teflon-valve NMR tubes at ambient probe temperature (298 K). ¹H and ¹³C NMR chemical shifts are reported in ppm relative to SiMe₄ and were determined by reference to the residual solvent resonances. Assignment of ¹³C NMR signals was made from 2D ¹H–¹³C HMQC and HMBC NMR experiments. ¹⁹F NMR chemical shifts were determined by external reference to an aqueous solution of NaBF₄. All coupling constants are given in hertz. Elemental analyses (C, H, N) were performed using a Flash EA1112 CHNS Thermo Electron apparatus and are the average of two independent determinations. Molecular weights of PLAs and PHBs were determined by size exclusion chromatography (SEC) at room temperature in THF on a Polymer Laboratories PL-GPC 50 plus apparatus (PLgel 5 μ m MIXED-C 300 \times 7.5 mm, 1.0 mL/min, RI and dual angle LS (PL-LS 45/90) detectors). The number average molecular masses (*M_n*) and polydispersity indexes (*M_w*/*M_n*) of the polymers were calculated with reference to a universal calibration vs polystyrene standards. *M_n* values of PLAs and PHBs were corrected with Mark–Houwink factors of 0.58 and 0.69, respectively, to account for the difference in hydrodynamic volumes between polystyrene and poly(lactide).^{19,23} The microstructure of PLAs was determined by homodecoupling

¹H NMR spectroscopy at 20 °C in CDCl₃ with a Bruker AC-500 spectrometer. The microstructure of PHBs was determined by analysis of the carbonyl region of ¹³C NMR spectra recorded in at 25 °C in CDCl₃ on a Bruker Avance AM-500 spectrometer.

NMR-Scale Generation of $\{\text{ON}^{\text{Et}}\text{NO}\}_2$ (1). Complex **1** was synthesized in situ from $\{\text{ON}^{\text{Et}}\text{NO}\}_2$ (20.0 mg, 0.029 mmol) and Y(N(SiHMe₂)₂)₃·2THF (18.5 mg, 0.029 mmol). A Teflon-valved NMR tube was charged with the solid reagents, and toluene (or benzene) (ca. 0.5 mL) was vacuum-transferred in at low temperature. The NMR tube was kept at –30 °C for 5 min. The released 1,1,3,3-tetramethyldisilazane was removed under vacuum at low temperature, and C₆D₅CD₃ (ca. 0.5 mL) was condensed into the NMR tube at –30 °C. The resulting solution of **1** was kept at –30 °C and analyzed by ¹H, ¹⁹F{¹H}, and ¹³C NMR spectroscopy, which revealed complete conversion of the reagents to **1**. ¹H NMR (300 MHz, C₆D₅CD₃): δ 0.27 (d, ³J = 3.0, 12H, NSiH(CH₃)₂), 1.43 (s, 6H, 2 CH₃), 1.57 (broad m, 4H, β -CH₂, THF), 2.65 (d, ²J = 14.7, 2H, CHHC=N), 2.77 (m, 2H, CHHCHH), 2.99 (d, ²J = 14.7, 2H, CHHC=N), 3.49 (m, 2H, CHH–CHH), 4.12 (broad m, 4H, α -CH₂, THF), 4.81 (sept, ³J = 2.9, 2H, NSiH(CH₃)₂). ¹⁹F{¹H} NMR (188 MHz, C₆D₅CD₃): δ –77.26 (q, ⁴J_{F–F} = 9.4, 6F), –78.84 (q, ⁴J_{F–F} = 9.4, 6F). ¹³C{¹H} NMR (HMBC/HMQC; 75 MHz, C₆D₅CD₃): δ 1.95 (NSiH(CH₃)₂), 3.72 (NSiH(CH₃)₂), 22.46 (CH₃C=N), 26.13 (β -CH₂, THF), 41.41 (CH₂C=N), 50.40 (CH₂N=C), 69.96 (α -CH₂, THF), 81.10 (C(CF₃)₂), 125.08 (q, ¹J_{C–F} = 266.4, CF₃), 175.50 (C=N).

$\{\text{ON}^{\text{Et}}\text{NO}\}_2$ (2). A solution of $\{\text{ON}^{\text{Et}}\text{NO}\}_2$ (40.0 mg, 0.058 mmol) in toluene (3 mL) was added dropwise to a solution of Y(N(SiHMe₂)₂)₃·2THF (37.0 mg, 0.058 mmol) in toluene (3 mL) at –30 °C over 2 min. Then, at the same temperature, a solution of (*R*)-(+)-*tert*-butyl lactate (8.0 mg, 0.058 mmol) in THF (1 mL) was added and the reaction mixture was kept at –30 °C. Colorless needlelike crystals of **3** were isolated from the reaction mixture after 15 h, washed with cold toluene (ca. 1 mL), and dried under vacuum (63.0 mg, 78%). ¹H NMR (500 MHz, THF-*d*₈): δ 1.31 (d, ³J = 7.0, 3H, OCH(CH₃)), 1.53 (s, 9H, C(CH₃)₃), 2.06 (s, 3H, CH₃), 2.16 (s, 3H, CH₃), 2.85 (d, ²J = 13.2, 2H, CHHC=N), 2.82 (d, ²J = 14.4, 2H, CHHC=N), 2.97 (d, ²J = 13.2, 2H, CHHC=N), 3.02 (d, ²J = 14.4, 2H, CHHC=N), 3.18 (m, 2H, CHHCHH), 3.62 (m, 4H, 2 CHHCHH), 4.85 (m, 2H, CHHCHH), 5.36 (q, ³J = 7.0, 1H, OCH(CH₃)). ¹³C{¹H} NMR (HMBC/HMQC; 75 MHz, THF-*d*₈): δ 20.67 (CH₃C=N), 21.95 (CH₃C=N), 21.36 (OCH(CH₃)), 27.36 (OC(CH₃)₃), 40.54 (CH₂C=N), 43.51 (CH₂C=N), 49.20 (CH₂N=C), 50.70 (CH₂N=C), 73.82 (OCH(CH₃)), 84.89 (OC(CH₃)₃), 82.17 (C(CF₃)₂) (only one signal observed, possibly two overlap), 125.49 (q, ¹J_{C–F} = 290.5, CF₃), 173.41 (C=N), 175.57 (C=N). ¹⁹F{¹H} NMR (188 MHz, THF-*d*₈): δ –77.98 (q, ⁴J_{F–F} = 9.4, 6F), –79.32 (q, ⁴J_{F–F} = 9.4, 6F), –81.06 (q, ⁴J_{F–F} = 9.4, 6F), –82.10 (q, ⁴J_{F–F} = 9.4, 6F). Anal. Calcd for C₄₂H₅₄F₂₄N₄O₁₀Y₂ (1408.67): C, 35.81; H, 3.86; N, 3.98. Found: C, 35.9; H, 3.7; N, 4.0.

$\{\text{ON}^{\text{Et}}\text{NO}\}_2$ (3). A solution of $\{\text{ON}^{\text{Et}}\text{NO}\}_2$ (20.0 mg, 0.029 mmol) in toluene (3 mL) was added dropwise to a solution of La(N(SiHMe₂)₂)₃·2THF (20.5 mg, 0.029 mmol) (or La(N(SiMe₃)₂)₃; 18.0 mg, 0.029 mmol) in toluene (3 mL) at –30 °C. The reaction mixture was stirred for 5 min at –30 °C. Volatiles were removed under vacuum, and the solid residue was washed with cold toluene (ca. 1 mL). Complex **3** was obtained as a white solid (24.0 mg, 70% from La(N(SiHMe₂)₂)₃·2THF or 22.0 mg, 65% from La(N(SiMe₃)₂)₃). Crystals of **3** suitable for X-ray diffraction were obtained by prolonged crystallization from a toluene solution at –20 °C. ¹H NMR (200 MHz, C₆D₅CD₃): δ 1.49 (s, 12H, CH₃), 2.61 (s, 8H, CH₂C=N), 3.07 (s, 8H, CH₂N=C), 12.46 (s, 1H, OH). ¹³C{¹H} NMR (HMBC/HMQC; 75 MHz, C₆D₅CD₃): δ 19.80 (CH₃), 44.98 (CH₂N=C), 51.55 (CH₂C=N), 81.40

(22) Anwander, R.; Runte, O.; Eppinger, J.; Gertberger, G.; Herdtweck, E.; Spiegler, M. *J. Chem. Soc., Dalton Trans.* **1998**, 847.

(23) Barakat, I.; Dubois, P.; Jerome, R.; Teyssie, P. *J. Polym. Sci., A: Polym. Chem.* **1993**, *31*, 505.

(C(CF₃)₂), 126.83 (q, ¹J_{C-F} = 313.9, CF₃), 168.63 (C=N). ¹⁹F{¹H} NMR (188 MHz, C₆D₅CD₃): δ -79.34 (s, 24F). Anal. Calcd for C₂₈H₂₉F₂₄LaN₄O₄ (1080.42): C, 31.13; H, 2.71; N, 5.19. Found: C, 31.3; H, 2.9; N, 5.2.

Crystal Structure Determination of 2 and 3. Crystals of **2** and **3** suitable for X-ray diffraction analysis were obtained by recrystallization of purified products (see above). Diffraction data were collected at 100 K using a Bruker APEX CCD diffractometer with graphite-monochromated Mo K α radiation ($\lambda = 0.71073$ Å). A combination of ω and ϕ scans was carried out to obtain at least a unique data set. The crystal structures were solved by means of the Patterson method; the remaining atoms were located from difference Fourier synthesis followed by full-matrix least-squares refinement based on F^2 (programs SHELXS-97 and SHELXL-97).²⁴ Many hydrogen atoms could be found from the Fourier difference analysis. Carbon- and oxygen-bound hydrogen atoms were placed at calculated positions and forced to ride on the attached atom. The hydrogen atom contributions were calculated but not refined. All non-hydrogen atoms were refined with anisotropic displacement parameters. The locations of the largest peaks in the final difference Fourier map calculation as well as the magnitude of the residual electron densities were of no chemical significance. Crystallographic data (excluding structure factors) for the structures in this paper have been deposited with the Cambridge Crystallographic Data Centre as Supplementary Publication Nos. 689843 and 689844 for **2** and **3**. Copies of the data can be obtained, free of charge, on application to the CCDC, 12 Union Road, Cambridge CB2 1EZ, U.K. (fax, +44-(0)1223-336033; e-mail, deposit@ccdc.cam.ac.uk).

Typical Procedure for *rac*-Lactide Polymerization (Table 4, Entries 11–17). In the glovebox, a Schlenk flask was charged with a solution of **2** (7.0 mg, 9.9 μ mol) in THF (1.0 mL). To this

solution was rapidly added solid *rac*-lactide (0.512 g, 3.55 mmol, 500 equiv vs Y) in THF (2.55 mL). The reaction mixture was stirred at 20 °C for 100 min. Small aliquots of the reaction mixture were periodically sampled with a pipet to determine the conversion by ¹H NMR spectrometry. The reaction was quenched by adding ca. 1 mL of acidic methanol (1.2 M HCl solution in CH₃OH), and the polymer was precipitated with excess methanol (ca. 3 mL). Then, the supernatant solution was removed with a pipet and the polymer was dried under vacuum to constant weight.

Typical Procedure for *rac*- β -Butyrolactone Polymerization (Table 4, Entries 22 and 23). In the glovebox, a Schlenk flask was charged with a solution of **2** (7.0 mg, 9.9 μ mol) in THF (0.17 mL). Into this solution was rapidly syringed in *rac*- β -butyrolactone (42.7 mg, 0.50 mmol, 50 equiv vs Y) with stirring. The reaction mixture was stirred at 20 °C for 15 h. After an aliquot of the reaction mixture was sampled with a pipet for determining the monomer conversion by ¹H NMR spectrometry, the reaction mixture was quenched by adding ca. 1 mL of acidic methanol (1.2 M HCl solution in CH₃OH). The polymer was precipitated with excess methanol (ca. 2 mL), the supernatant solution was removed with a pipet, and the polymer was dried under vacuum to constant weight.

Acknowledgment. This work was financially supported in part by the *Agence Nationale de la Recherche* (Grant No. ANR-06-BLAN-0213; grant to E.G.) and Total Petrochemicals (grant to E.K.). J.-F.C. gratefully thanks the *Institut Universitaire de France* for a Junior IUF fellowship (2005–2009).

Supporting Information Available: Figures giving 1D and 2D NMR spectra for complexes **1–3** and CIF files giving crystal structure data for **2** and **3**. This material is available free of charge via the Internet at <http://pubs.acs.org>.

OM800611C

(24) (a) Sheldrick, G. M. SHELXS-97, Program for the Determination of Crystal Structures; University of Göttingen, Göttingen, Germany, 1997. (b) Sheldrick, G. M. SHELXL-97, Program for the Refinement of Crystal Structures; University of Göttingen, Göttingen, Germany, 1997.